The Lightcurve and Colors of Unusual Minor Planet 1996PW

John K. Davies

Joint Astronomy Centre, 660 N A'ohoku Pl., Hilo, Hawaii, 96720, USA

E-mail: JKD@jach.hawaii.edu

Neil McBride, Simon F. Green

Unit for Space Sciences & Astrophysics, School of Physical Sciences

University of Kent, Canterbury, CT2 7NR, UK

Stefano Mottola, Uri Carsenty

DLR, Institute of Planetary Exploration, D-12489 Berlin, Germany

Devinder Basran

Joint Astronomy Centre, Hilo, Hawaii

(present address Dept of Physics, University of Victoria, Canada)

Kathryn A. Hudson and Michael J. Foster

Unit for Space Sciences & Astrophysics, School of Physical Sciences

University of Kent, Canterbury, CT2 7NR, UK

March 19, 1998

Number of pages (inc Figs. and Tables): 32

Text: 18 pages

Tables (including footnotes): 8

Figures: 6

Keywords:Asteroids, Rotation, Photometry, Infrared, Comets

Suggested running head: Lightcurve and colors of 1996PW

Correspondence and proofs to:

Dr J.K. Davies

Joint Astronomy Centre

660 N A'ohoku Pl.

Hilo

Hawaii 96720, USA

tel: 808-969-6524

e-mail JKD@JACH.Hawaii.edu

Abstract

Minor Planet 1996PW is unusual in having the orbital characteristics of a long period comet but showing no sign of cometary activity around the time of its discovery. We present optical data which reveals a double peaked lightcurve (period 35.44±0.02 hrs and amplitude 0.44±0.03 magnitudes) and VRIJHK photometry which shows colors (V−R=0.56±0.04, V−I=1.03±0.06, V−J=1.80±0.05, V−H=2.19±0.05 and V−K=2.32±0.05) typical of those of D type asteroids and suspected 'bare' comet nuclei. A low signal to noise reflectance spectrum in the K band shows a flat continuum with no evidence for spectral features. Image profiles from co-added frames in the R band indicate no apparent cometary activity with an implied upper limit to the dust production rate of 0.03 kg s^{-1}.

1 INTRODUCTION

Minor planet 1996PW was discovered at the NEAT telescope on 1996 August 9th (Helin *et al.* 1996) and its unusual orbit was identified by Williams (1996). With an eccentricity of >0.99, a perihelion distance of 2.54 AU and inclination 30° the orbit of 1996PW is similar to that of a long period comet, yet Jewitt (1996) reported no evidence for a coma in images taken on 1996 Aug 16. Rabinowitz (1996) summarised optical photometry from which mean reflectance colors consistent with the spectra of S or D type asteroids were deduced, and Hammergren (1996) reported that a low resolution spectra of 1996PW was featureless with a red sloping continuum consistent with cometary nuclei and D-type asteroids. Williams *et al.* (1996) reported B and R magnitudes taken on 1996 Sept 2–4.

We obtained optical and infrared photometry and infrared spectroscopy in the period August–October 1996. Preliminary analysis (Mottola & Carsenty 1996) of the September lightcurve indicated a rotation period of ∼35.5 hours and a lightcurve amplitude of ∼0.4 magnitudes. Additional optical photometry was carried out in October 1996 to refine the optical colors and to refine the lightcurve parameters so that the non-simultaneous optical and infrared data could be combined for comparison with other outer solar system objects.

2 OBSERVATIONS AND DATA REDUCTION

2.1 ESO/Bochum lightcurves

Optical photometry was carried out on 1996 Sep 7–10 from ESO, La Silla with the 60 cm Bochum telescope, the DLR MkII CCD camera, and a 1024×1024 pixel thinned Tektronix chip (image scale 0.52 arcsec per pixel). Most of the ESO observations were made with an R filter, but standard stars and two 1996PW frames were measured in the Johnson V band. Conditions were photometric on all 4 nights and during the observations the telescope was tracked at the object's rate. The CCD frames were bias corrected and then flat fielded using twilight flats. Intensity was extracted using Astphot, a synthetic aperture photometry computer program developed by SM at the DLR. On-line reduction of the photometric data allowed the lightcurve variation to be followed in real time in order to continue the observations until the rotation period was secured. Relative lightcurves in the R band were obtained on each night, and absolute calibration of V photometry was performed using GSPC-1 stars (Lasker, Sturch *et al.* 1988). Observational details are given in Table I.

2.2 INT optical photometry

Optical photometry was carried out on 1996 October 11–13 from the Observatorio del Roque de Los Muchachos, La Palma, using the 2.5 m Isaac Newton Telescope (INT) and a CCD camera, fitted with a TEK3 1024×1024 thinned chip, at prime focus. Frames were taken with Kitt Peak VRI broadband filters (equivalent to the Johnson V and Kron-Cousins RI photometric system) at an image scale of 0.59 arcsec per pixel. Observations in the VRI filters were made on each night. Since autoguiding was only possible for fixed sources the telescope was tracked at the sidereal rate, resulting in image trailing of 1.7 arcsec on 1996PW during a typical 300 second exposure. The observations were bias corrected and flat fielded using the Starlink software package KAPPA (Currie 1992). Flat field frames were obtained using de-focused images of the uniformly illuminated dome interior.

Photometric calibration was performed using equatorial standard fields PG 2331 and PG 0231 (Landolt 1992) providing Kron-Cousins standard magnitudes. Although on each night the sky appeared to be clear, there were several occasions of high and rapidly changing humidity on the first and third nights. Fortunately the motion of 1996PW was such that approximately one quarter of the area of fields taken on consecutive nights overlapped. By using relative photometry of stars common to pairs of frames, it was possible to normalise all the data to the second night. The photometry was performed using the Starlink Photom aperture photometry package (Eaton 1989) with apertures of 6 arcsec (10 pixels) diameter. The absolute calibration was then performed by reference to object frames and standard star images taken on the second night. Observational details are given in Table I.

2.3 UKIRT infrared photometry

Infrared imaging was obtained on 1996 September 4, 10, 12 and October 23, 29, 30 with the infrared camera IRCAM on the UK Infrared Telescope, UKIRT. The camera, which is equipped with a 256×256 InSb array, has a plate scale of 0.286 arcsec per pixel and a field of view of 73.2 arcsec. During each observation, the object was tracked by moving the telescope at the predicted rate of the asteroid's motion. The identification of the target was confirmed by noting its movement relative to faint background stars either immediately in the TV guide camera or subsequently in the reduced images.

An IRCAM image for a given filter comprised a mosaic of several separate frames each of which was background limited and offset slightly from the others to minimise the effect of bad pixels. After subtracting an appropriate dark from each frame of the mosaic, frames in each filter were median filtered to produce a flat field. The individual frames were then divided by this flat field and co-added in the reference frame of the asteroid. The September 10th K observations were unsuitable for median filtering due to the small number of positions observed, so on this occasion a flat field was constructed from other frames made in the same filter on the same night. Magnitudes were extracted using 5 arcsec apertures on the images and calibrated via images of UKIRT faint standard stars observed at similar airmasses and times. The quoted errors include statistical uncertainties in the images with uncertainties in photometric calibration.

The UKIRT observations on 1996 October 29 and 30 were made in conditions which were clearly not photometric due to the presence of cirrus clouds. These were calibrated relative to other stars in each target field which were observed under photometric conditions on October 31 by T.R. Geballe. For this relative photometry, separate images were constructed with respect to both the object and sidereal frames of reference before the aperture photometry was carried out. Observational details are given in Table I.

2.4 UKIRT infrared spectroscopy

The infrared spectroscopy was obtained with the UKIRT Cooled Grating Spectrometer (CGS4) on 1996 August 23 and September 29. At the time of the observations the instrument was configured with its 150 lines mm^{-1} grating and its short focal length camera which provides a spectral range of approximately 0.16 μm per grating setting at a resolution of the order of 3000. This configuration is not ideal for detecting the broad, shallow spectral features sometimes seen in outer solar system objects and so on each occasion two wavelength settings, selected to cover the deep absorption at 2.25 μm seen in 5145 Pholus (Davies *et al.* 1993a), were used. The two settings had considerable overlap to allow the joining of the two spectral fragments and the resulting spectra covered the region 2.165 to 2.42 μm. For each configuration, an observation was also made of a nearby main sequence G star at similar airmass in order both to remove the effects of telluric absorptions and to allow the production of a reflectance spectrum directly. The stars used were BS8917 (G0V) and BS8883 (G4V).

The CGS4 spectra were reduced in the standard manner for this instrument. Each image was divided by a flat field taken using CGS4's internal black body followed by construction of object-sky pairs from consecutive observations nodded along the slit. The object-sky pairs were added to make a final 2D spectral image. This was corrected for the curvature of the image resulting from the CGS4 optics by using the signal from a bright star to map the distortion across the array and resampling the data to remove the distortion. The rows containing the asteroid spectra were extracted from the image and wavelength calibrated using arc lines from the internal calibration argon lamp. The resulting spectra were divided by the spectrum of a G star observed in an identical instrument configuration and reduced in the same way.

The two spectral fragments for each night were normalised so that the ratio at 2.2 μm was equal to 1.0 and the second fragment overlapped the first. The resulting spectrum was then rebinned into 64 bins to improve the signal to noise ratio. Examination of the spectra showed that the signal to noise ratio of the data from August 23 was better than that for September 29 and so the two spectra were then added giving a weight of 1.5 to the August data. Observational details are given in Table I.

3 RESULTS

3.1 Lightcurve of 1996PW

The lightcurve and period of 1996PW are defined predominantly by the ESO/Bochum observations in the R band which was used as it matched better the sensitivity characteristics of the DLR camera. Due to the lack of suitable R band standard stars in the vicinity of the asteroid, a calibration was performed by acquiring two data points in the Johnson V band, and then calibrating them against a GSPC-I star. These data points, obtained on the 2nd and 4th night of the ESO observations (at lightcurve phase 0.396 and 0.760 respectively) define the overall level of the lightcurve. Conversion of R data into a V lightcurve was performed assuming that there are no gross color changes over the asteroid's surface, as indicated by the INT color data (see section 3.4).

All ESO magnitudes for period determination have been corrected to $r = \Delta = 1$ AU, and to the phase angle of 1996 Sept 8.0 (7.6°) using a G parameter of 0.05 (see section 3.2). The lightcurve period was calculated by a procedure which fits a fourier series to find the period and magnitude shifts of independent data sets which produce the smallest residuals. A 6th order fit was used in the manner described by Harris *et al.* (1989). Treating the 4 nights' data independently and allowing the fitting program to shift the data sets to produce the lowest residuals, resulted in nights 2, 3 and 4 needing no relative magnitude shift and night 1 needing only a 0.02 magnitude shift (in order to overlay the night 4 data near phase 0.75). Thus confidence in the overall photometric calibration is high.

Although the September ESO data gave the initial definition of the period, the October INT data in the V band was then also incorporated to determine the period over a greater timebase. The INT data were converted to $r = \Delta = 1$ AU, and to the phase angle of 1996 Oct 13.0 (17.9°) using a G parameter of 0.05 (see section 3.2). The final composite lightcurve is shown in Fig. 1a. The period of 1996PW is found to be 35.44±0.02 hr with a lightcurve amplitude of 0.44±0.03 magnitudes (at a phase angle of 7.6°) defined exclusively by the ESO data. Over the $\sim$1 month interval between the ESO and INT observations the change in viewing and illumination is sufficiently large to result in changes in the amplitude and detailed shape of the lightcurve. However, the lightcurve fits to the INT data (Fig. 1b) demonstrate that the overall shape is sufficiently similar for these data to be used to constrain the period. Observational details are given in Table II.

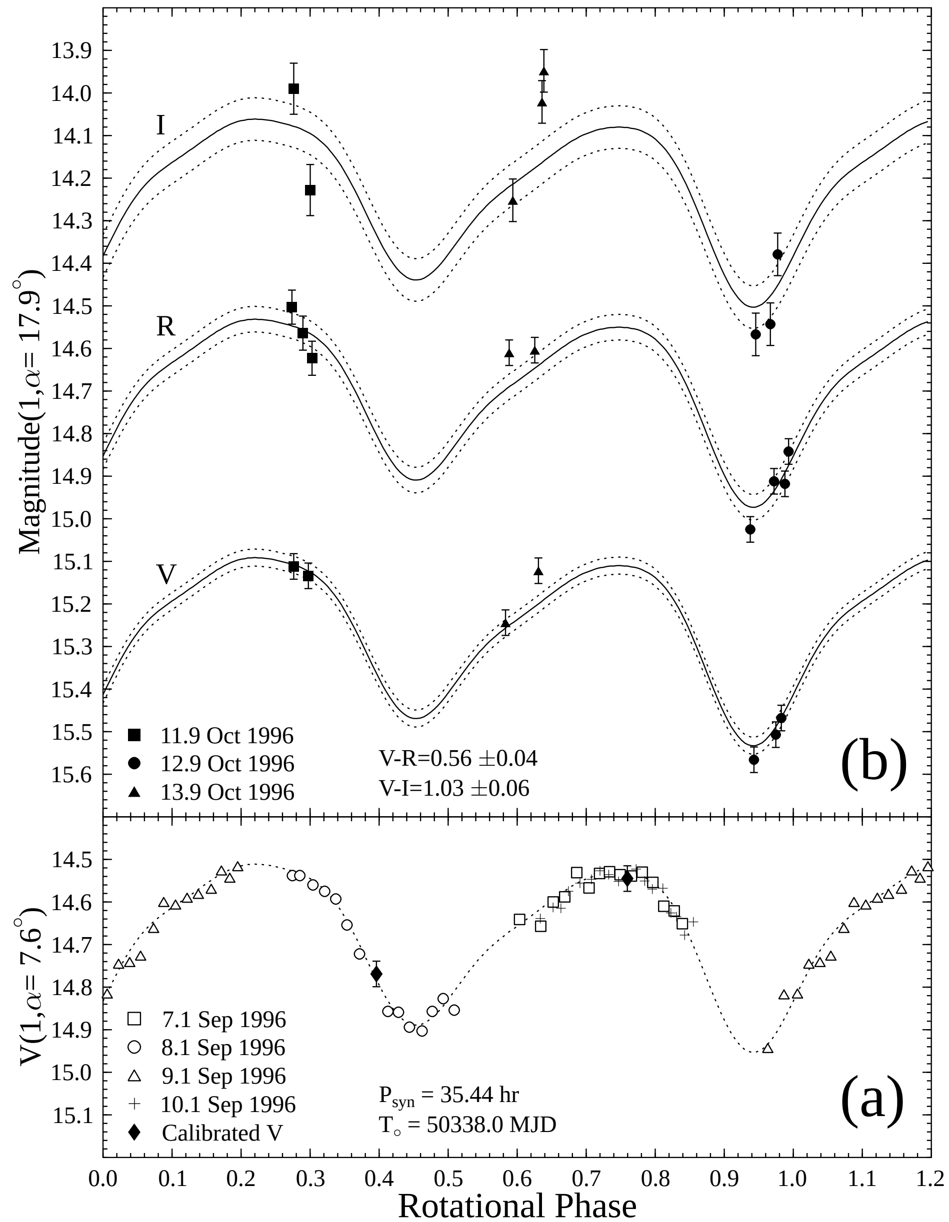

Figure 1: Lightcurve of 1996PW. (a) The composite 'visual' lightcurve determined from ESO Bochum R data (open symbols) fitted to calibrated V photometry (filled symbols). The period is obtained using a 6th order fourier fit (dotted line). (b) INT photometry in V, R and I bands, compared with the lightcurve from (a) shown as a solid line, with estimated upper and lower bounds shown as dotted lines.

3.2 Phase curve

To deduce the G parameter and absolute magnitude it is desirable to observe an object over a large range of phase angles and, although for 1996PW the data are limited, some estimates can be made. Suitable data currently available are the Bochum V data from September 8 and 10, the INT data from October 11–13, R data from Williams *et al.* (1996) and V data from Rabinowitz (1996). These were corrected to $r = \Delta = 1$ AU, the rotational phase of each observation was determined, and a lightcurve correction applied to the photometry to obtain the *mean* V(1,α) magnitude (defined as being mid-way between the lightcurve maximum and minimum) assuming that the derived lightcurve shown in Fig. 1 was applicable for the whole observation period. The V$-$R colour derived from the INT observations was used to convert the Williams *et al.* data to V magnitudes. Errors are estimated from a combination of the quoted photometric errors (assumed $\pm$0.05 for Williams *et al.* data), uncertainties in the lightcurve phase and colour corrections.

Fig. 2 shows the data plotted with phase curves defined by different G parameters fitted through the data. The best fit to just the INT and Bochum data gives G=$-$0.14. Even allowing for the larger observational errors of the small phase angle data, the G parameter value can be no larger than $-$0.05 to give a reasonable fit through all the data. Although a negative value of the G parameter is not unphysical, values less than zero are not normally encountered among the asteroid population. It is possible that the lightcurve amplitude corrections are under-estimated for the large phase angle data (and slightly over-estimated for the small phase angles) which would result in a slightly higher G parameter value. Alternatively, a low level of cometary activity might be present. The smaller phase angle data were taken closer to perihelion and so it is possible that the G parameter might have (a more 'normal') >0.0 value, but with some cometary activity 'brightening' the phase curve at the lower phase angles. If this were the case then the coma contribution must be small enough not to be identified in imaging data (no coma was reported by Rabinowitz or Williams *et al.*). If there is no coma contribution in the INT data then the brightening would be 0.15 magnitudes for the Bochum data and somewhat larger for the earlier data. We can assess whether the presence of coma at this level would produce an observable difference between the image profile of 1996PW and a star in one exposure by considering a simple outflow model and comparing it with observed image profiles. This is described in the next section. In the absence of further data to define better the phase curve, we can only infer a low value of G, consistent with low albedo objects. We have assumed G=0.05 when preparing the composite lightcurve data (although the corrections for phase angle over a given data set are very small and so the precise value of G is relatively unimportant). Based on the fits shown in Fig. 2, we estimate the absolute magnitude of 1996PW to be H=14.1$\pm$0.1.

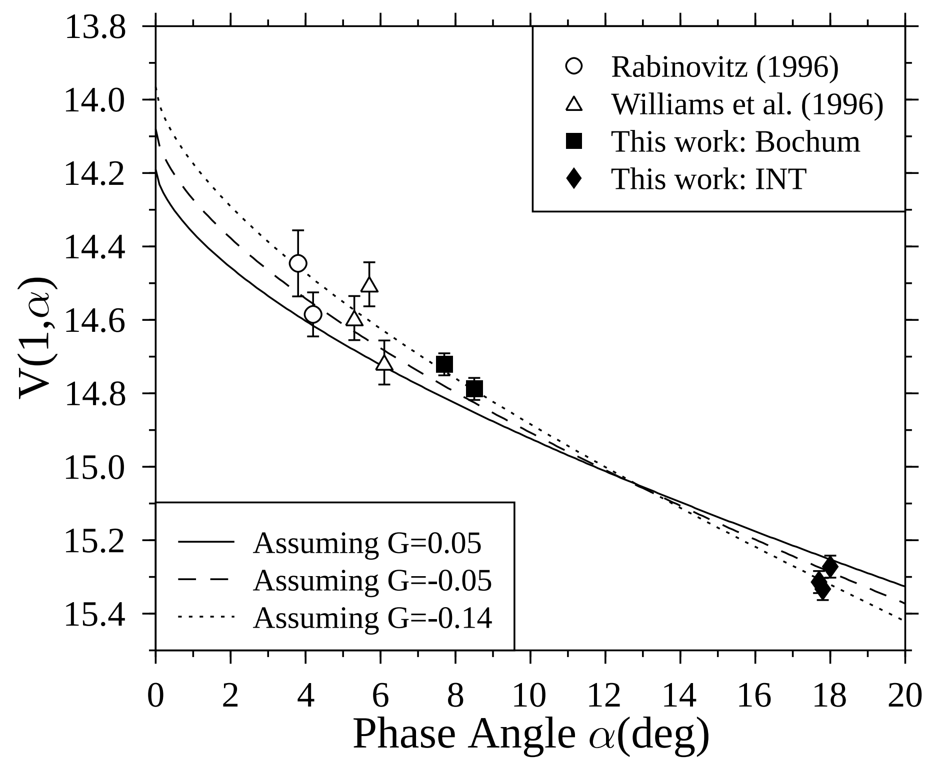

Figure 2: Phase curve of 1996PW. Trial fits are shown using different G parameters. See text for details.

3.3 Search for activity

In order to search for any cometary coma around 1996PW, the nine R band frames taken with the INT were coadded in the object's reference frame. The INT was autoguided at the sidereal rate so that tracking on stars was very good, and the trails produced by the motion of 1996PW during the exposures were well defined. The more numerous ESO/Bochum frames were tracked on the target but the Bochum telescope suffered from a periodic tracking error when tracking non-sidereally and so the resulting images were not trailed in a predictable and repeatable fashion. Although this did not affect the aperture photometry, it makes comparisons between precise target and star profiles unreliable and just the INT frames were used for the coma investigation.

We measured the profile of 1996PW using pixels that were within a sector $\pm 10°$ from a line centered on the object and perpendicular to 1996PW's motion on the frames. The profiles were also determined for 4 field stars, 3 of which were similar in brightness to 1996PW and the other $\sim$2 mags brighter. The total exposure time for the coadded INT R frames was 3140 s. The sky background was defined for each co-added image using the modal sky value at a distance of between 15 and 17 pixels (8.9–10.0 arcsec) from the peak where no contribution from the object was apparent.

Fig. 3 shows the profiles converted to sky-subtracted surface brightness as a function of projected distance from the target (pixels within a distance of 3 pixel diameters are plotted individually, with mean values at larger distances). The test star profiles have been normalised to the 1996PW profile at the distance of 1 pixel, and have somewhat smaller 1 sigma error bars (not plotted for clarity). The profiles appear identical within 4 arcsec, but some divergence is apparent further from the 'nucleus'. The scatter in the star profiles is significantly larger than the statistical errors. This may be due to faint background objects which contribute to the star profile (these are not accounted for in the modal background determination). Because the profiles in Fig. 3 are normalised near their peak (at 1 pixel), the effect of background objects in the wings will be proportionately less important for a brighter object, as is apparent for test star 1. The 1996PW profile appears to have rather more contribution in the wings compared with the other test stars of similar brightness. This may be due to a faint coma, but if the scatter in the star profiles is indicative of the uncertainties in the point spread function due to faint background objects, then we cannot confidently conclude that there is any significant coma present.

We can however determine nominal dust production rates of 1996PW based on comparison with each of the test star profiles, which can provide an estimated upper limit of the dust production rate. We assume a spherically symmetric coma for 1996PW with a constant outflow velocity and a single grain size. We obtain the surface brightness B of a pixel by integrating along the line of sight:

$$B = a^2 \int_{-\infty}^{\infty} F(d) \;\; dx \tag{1}$$

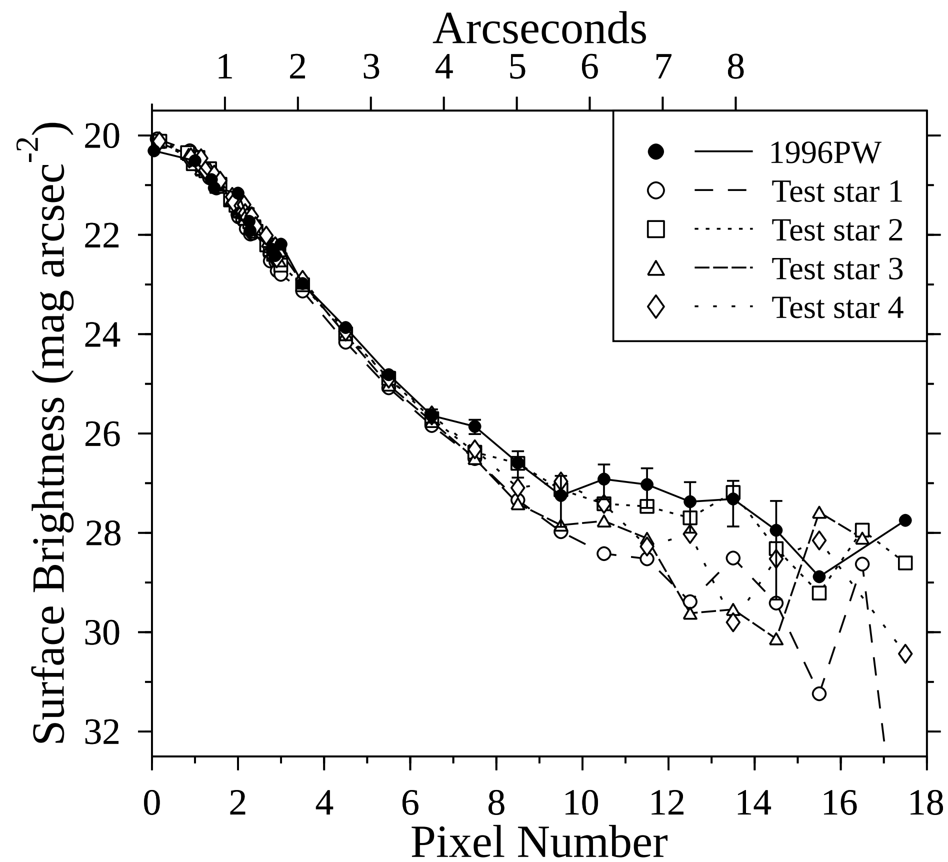

Figure 3: Surface brightness profile of 1996PW compared with field stars. Each object is a composite of 9 R frames, see text for details.

where x is the distance along the line of sight (and is zero at a point nearest the nucleus), d is the distance from the nucleus of a unit volume which contributes a flux $F(d)$, and a is the projected pixel width in the plane of the sky. It is clear that

$$\frac{F(d)}{F_\circ} = \frac{r_\circ^2}{d^2} \tag{2}$$

where $r_\circ$ is the projected distance of a pixel from the object centre (in the plane of the sky) and $F_\circ$ is the flux contribution from a unit volume at that projected distance. Hence

$$B = a^2 \int_{-\infty}^{\infty} \frac{F_\circ r_\circ^2}{x^2 + r_\circ^2} \; dx \quad = \quad a^2 F_\circ r_\circ \pi \quad . \tag{3}$$

The flux $F_\circ$ is given by

$$F_\circ = N \; A \; \frac{S_\circ}{r^2} \; \frac{R^2}{\Delta^2} \tag{4}$$

where N is the grain spatial number density, and A is the geometric albedo (at this phase angle), $S_\circ$ is the Solar constant (1430 W m$^{-2}\mu$m^{-1} in the R band), r is the heliocentric distance of the comet (in AU), R is the grain radius (in m), and Δ is the comet–Earth distance (in m). Thus we can combine Eqs. (3) and (4) to solve for N. If we assume a coma composed of grains of only one size, then the dust mass loss rate is

$$\dot{M} = N \; \frac{4}{3} \pi R^3 \; \rho \; V_t \; 4\pi r_\circ^2$$

where V$_t$ is the dust grain terminal velocity and ρ is the grain bulk density. The $4\pi r_\circ^2$ term represents the integration over the whole spherical shell (of unit thickness) at a projected distance $r_\circ$. This becomes

$$\dot{M} = \frac{16\pi}{3} \; \frac{\Delta^2}{a^2} \; \frac{r^2}{S_\circ} \; \frac{B \; R \; \rho \; V_t \; r_\circ}{A}$$

noting that independent determinations of $\dot{M}$ can be obtained for each pixel distance (*i.e.* representing different $r_\circ$ distances).

For the INT observations of 1996PW, $\Delta = 2.87 \times 10^{11}$ m, $a = 8.22 \times 10^5$ m, $r = 2.63$ AU, and our photometric calibration yields $B = c \times 4.92 \times 10^{-22}$ W m^{-2} μm^{-1}, where c is the counts from the coma (*i.e.* 1996PW profile minus star profile). We assume $R = 0.5 \times 10^{-6}$ m, $\rho = 1000$ kg m^{-3}, $V_t = 0.4$ km s^{-1}, and $A = 0.05$.

Table III shows the production rates ($\dot{M}$) derived from each pixel range individually, for each test star. If the brighter star (test star 1) represents the true point spread function, and 1996PW has no contamination from faint background objects, the dust production rate is $\sim$30 g s^{-1}, which is several orders of magnitudes below that of a typical 'inactive' comet at this heliocentric distance.

This upper limit is clearly dependent on the assumed values of R, ρ, V_t and $1/A$. Values of R = 0.1–2.5$\times$10^{-6} μm, ρ = 300–3000 kg m^{-3}, V_t = 100–800 m s^{-1}, and A = 0.2–0.03 yield upper limits to the dust production rate in the range 0.1 to 2000 g s^{-1}.

3.4 VRI Colors

Conditions during the La Palma observations were not reliably photometric on each night and this creates some uncertainty in deriving VRI colors from these data. The method adopted was to take the lightcurve of Fig. 1a and adjust it in magnitude until it fitted the La Palma data for each color (Fig. 1b). In principle the magnitude offset required to fit the V data reflects the difference in phase angle between the La Palma and ESO data. The additional differences required to fit the other two filters to the V lightcurve are due to the V$-$R and V$-$I colors.

Although this method is not rigorous, since the ESO and La Palma observations were made at different phase angles ($\sim$8° and $\sim$18° respectively) which might be expected to introduce a change in lightcurve amplitude of up to 20% and it assumes no colour change with phase, it has the benefit of using all the data to determine mean colors. From Fig. 1b there is an indication that the October 13.9 data are slightly divergent from the September lightcurve which fits the October 11 and 12 data. However, the time intervals between the observations in different filters on each night were small and there is no evidence from Fig. 1b of any *change* in color with phase within the observational errors.

We derive mean colors V$-$R=0.56$\pm$0.04 and V$-$I=1.03$\pm$0.06. The quoted errors reflect the uncertainty in fitting the September lightcurve through each of the October V, R and I datasets (upper and lower limits shown as dotted curves in Fig. 1b). Each individual data point has 1 sigma error bars displayed, and therefore colors derived from specific pairs of frames would have considerably larger errors. Rabinowitz quoted mean *reflection* colors (*i.e.* the object color minus the solar color) of V$-$R=0.19$\pm$0.04 and V$-$I=0.34$\pm$0.03. Using solar colors of 0.36 and 0.71 respectively (Meech *et al.* 1995), we translate these to V$-$R=0.54 and a mean V$-$I=1.05 which are in good agreement with our result. Observational details are given in Table IV.

3.5 VJHK Colors

Determination of optical to infrared colors requires a V magnitude at the time of the UKIRT observations. The rotational phase was calculated for the mid-frame time of each UKIRT observation. In the case of the September data, a V(1,α) was taken from the lightcurve of Fig 1a and corrected for the small changes in heliocentric distance, geocentric distance and phase angle (using a G value of 0.05). Since the differences in solar phase angle during this time interval were small, even a significant error in the value of G would have only a small effect on our deduced V magnitude. In the case of the infrared photometry taken in October a V magnitude was estimated in a similar manner using the V lightcurve plotted in Fig. 1b.

All of the optical–IR colors deduced in this manner are listed in Table V which includes the values used during the intermediate steps. The resulting average values are V$-$J=1.80$\pm$0.05, V$-$H=2.19$\pm$0.05, V$-$K=2.32$\pm$0.05. Quoted uncertainties comprise the random photometric errors, and the systematic uncertainties in the V calibration. Observational details are given in Table V.

4 DISCUSSION

The high eccentricity of 1996PW is strongly suggestive of an origin in the Oort cloud so it is natural to compare its properties with those of comet nuclei and distant minor planets such as the Centaurs and Kuiper Belt objects.

We were not able to observe 1996PW in the thermal IR and so cannot determine its albedo directly, but the low G parameter ($\leq$0.05) indicated by the phase curve implies a low albedo. Assuming a geometric albedo of 0.05 the absolute magnitude H=14.1$\pm$0.1 indicates a diameter of 10 km, which is not unreasonable for a cometary nucleus, but there is no direct evidence for any significant dust coma from the co-added INT data. For a dust production rate of 0.03 kg s^{-1} the coma contribution to the 6 arcsec (radius) aperture used for the INT data (V$\sim$18.9) is 0.017 magnitudes. In order to produce the 0.15 magnitude enhancement in the low phase angle data (V$\sim$17.7) to explain the negative G parameter from the phase curve (Fig. 2), a dust production rate of 0.9 kg s^{-1} is required. Although this would have resulted in an easily identifiable coma in the co-added INT data, it would not have been apparent in the Bochum data due to the poor tracking and probably would not have been seen in the earlier individual frames from Rabinowitz and Williams *et al.* due to the lower signal to noise.

Having established the likely absence of a coma around 1996PW, it is natural to compare its colors with those of comets for which activity was absent or at a low level at the time of observation, allowing the nucleus to be detected. Suitable data (See Table VI) are from comets 1P/Halley at 4.8 AU from the Sun (Cruikshank *et al.* 1985; Thomas and Keller 1989), 29P/Schwassmann-Wachmann 1 during a quiescent phase (Hartmann *et al.* 1982), 49P/Arend-Rigeax (Millis *et al.* 1988; Luu 1993), 28P/Neujmin 1 (Campins *et al.* 1987; Jewitt and Meech 1988), the comet-asteroid transition object 4015 Wilson-Harrington when it was reportedly asteroidal (Hartmann *et al.* 1982; Campins *et al.* 1995) and 2060 Chiron when it was relatively inactive (Hartmann *et al.* 1982; Hartmann *et al.* 1990). The JHK data of Campins *et al.* (1995) for 4015 (J$-$H=0.29$\pm$0.11, H$-$K=$-$0.04$\pm$0.12) support the J$-$H color of 4015 given by Hartmann *et al.* (1982) but give an H$-$K that is significantly less red (if this were to be the case then the V$-$K of 4015

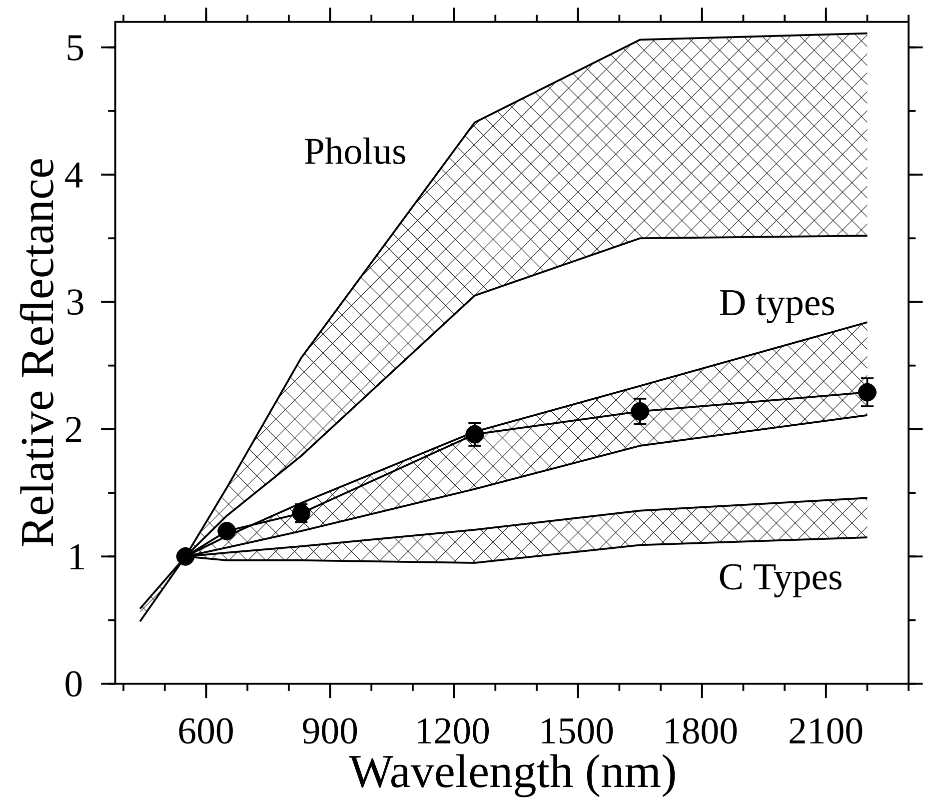

Figure 4: Relative reflectance spectrum of 1996PW (solid symbols) compared with C and D type asteroids and the Centaur Pholus. The shaded regions for the C and D type asteroids represent the range of typical values for the class (Hartmann *et al.* 1990). The range shown for Pholus is defined by the errors in photometry given in Table VI. We assume solar colors of V−R=0.36, V−I=0.71 (Meech *et al.* 1995), V−J=1.07, V−H=1.36 and V−K=1.42 (Degewij *et al.* 1980).

might be as low as 1.3). Values for Neujmin 1 are based on the spectral reflectances of Campins *et al.* (1987) converted by us back into VJHK colors. In addition to 2060 Chiron we consider three Centaurs for which optical–IR colors have been published (Davies *et al.* 1996; Weintraub *et al.* 1997) and the bright Kuiper Belt object, 1993SC (Davies *et al.* 1997).

The infrared colours and low albedos of the cometary nuclei are similar to those of D type asteroids prevalent in the outer solar system. The optical–IR colors of 1996PW, and the implied low albedo from the phase curve, are similar to these 'traditional' comet nuclei and D type asteroids (and rule out an S type classification; a possibility if using only optical photometry). Fig. 4 shows the relative reflectance spectrum of 1996PW, compared with typical dark asteroids (C and D types) and the Centaur 5145 Pholus. However, the situation is clearly not simple, since 4015 Wilson-Harrington and Centaur 2060 Chiron, both of which can have cometary activity are significantly less red than other comets. Those Centaurs which show no activity have similar colors to 1996PW (1995GO) or are more red (5145 Pholus,

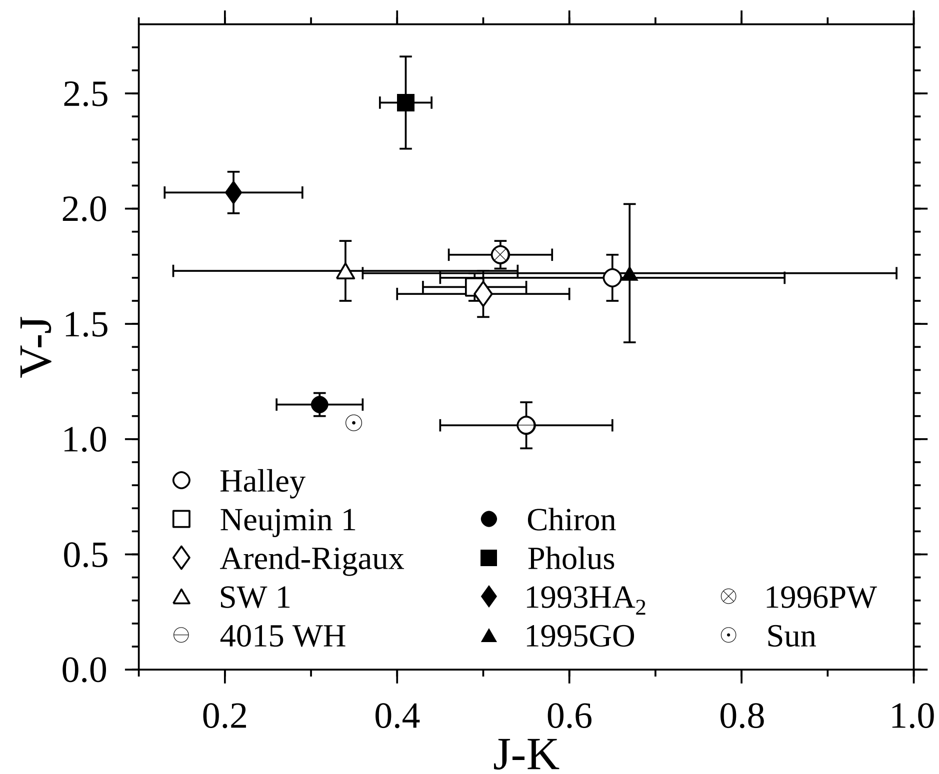

Figure 5: VJK color-color diagram of 1996PW, cometary nuclei and Centaurs.

7066 Nessus) as is the Kuiper Belt object 1993SC. Fig. 5 illustrates the visual–IR colors of these objects. Color differences may reflect differences in surface composition and/or the nature of the scattering surface (*e.g.* grain size and shape). Hartmann *et al.* (1990) argued that 2060 Chiron is an ice-rich object which has only recently arrived in the solar system while 4105 Wilson-Harrington (which has similar colors) has presumably been almost deactivated during its period in the inner solar system. Luu *et al.* (1994) suggest that Chiron is covered by a rubble mantle (grains too large to be ejected by the gas drag from the sublimation of volatiles). Although the observed cometary nuclei are assumed to have similar mantles over much of their surfaces, they are generally active at smaller heliocentric distances than Chiron, which would result in the surfaces having a different grain size distribution and so perhaps different colors.

7066 Nessus, 5145 Pholus and 1993SC have not to date shown cometary activity and are favoured candidates for objects retaining irradiation mantles formed by bombardment of their surfaces by high energy particles over the lifetime of the solar system. No infrared spectroscopy has been reported for 7066 Nessus but 5145 Pholus has an unusual IR spectrum (Davies *et al.* 1993a; Luu *et al.* 1994) with an absorption feature at 2.25 μm which is approximately 0.1 μm wide and at its minimum has a flux approximately 70% of the flux at 2.2 μm. Although the UKIRT spectrum of 1996PW shown in Fig. 6 is quite noisy, it is clear that no feature of this depth could be present.

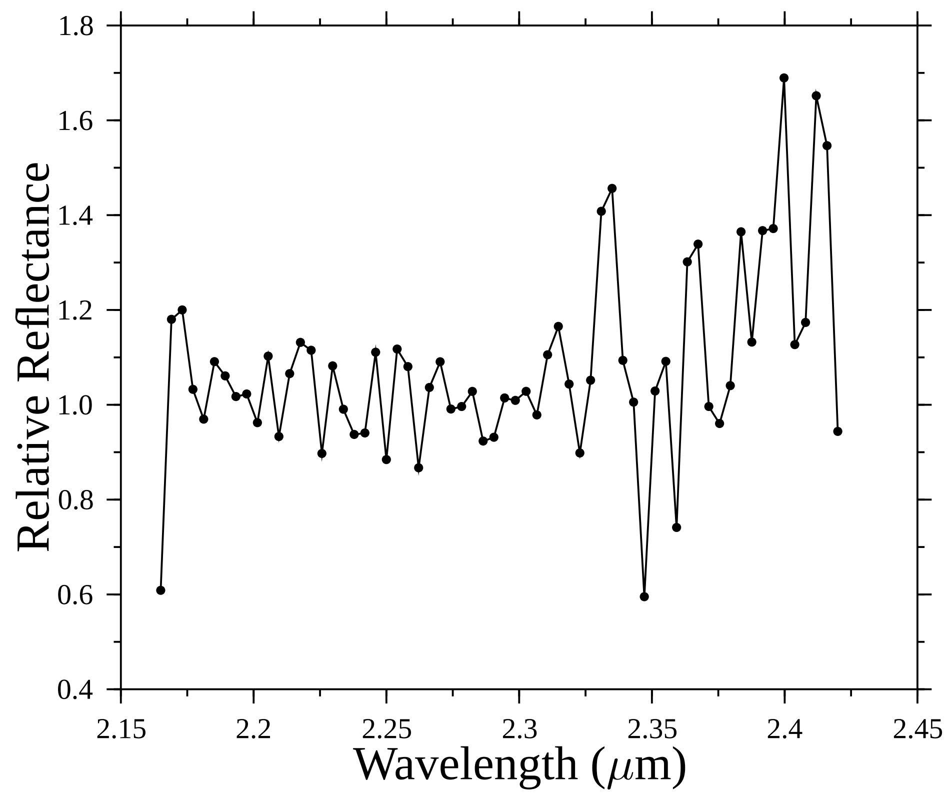

Figure 6: The K band infrared spectrum of 1996PW. Errors are commensurate with the scatter in the data.

5 CONCLUSIONS

We find that 1996PW has a rotation period of 35.44±0.02 hours and amplitude of 0.44±0.03 magnitudes. The G parameter appears to be low ($\leq$0.05) which implies a low albedo. Assuming a geometric visual albedo of 0.05, the diameter is 10 km. There is no compelling evidence for cometary activity. The visual and infrared colors of 1996PW are consistent with D type asteroids and comet nuclei observed when quiescent. We conclude that 1996PW is what might generally be regarded as the nucleus of a long period comet which was not significantly active during its 1996 perihelion passage.

ACKNOWLEDGEMENTS

UKIRT observations of 1996PW were made both during the UKIRT Service Observing Programme and as a target of opportunity during scheduled runs. We thank in particular S.K. Leggett, T. Kerr, T.G. Hawarden, L. Miller, T.R. Geballe and the UKIRT telescope operators for their co-operation in making these observations. We also thank the support staff of the INT for their assistance during the regularly scheduled observing at La Palma. The Isaac Newton telescope is operated on the island of La Palma by the Royal Greenwich Observatory in the Spanish Observatorio del Roque de los Muchachos of the Instituto de Astrofisica de Canarias. UKIRT is operated by the Joint Astronomy Centre on behalf of the Particle Physics and Astronomy Research Council (PPARC). Image processing and data reduction were performed using the STARLINK network and software. STARLINK is funded by PPARC. N. McBride, K. Hudson and M. Foster acknowledge the financial support of PPARC. We thank the two referees for positive and constructive comments which have improved the manuscript

REFERENCES

Altenhoff W.J. and P. Stumpff P. 1995. Size estimate of asteroid 2060 Chiron from 250 GHz measurements. *Astron. & Astrophys.* **293**, L41–L42.

Binzel R.P. 1992. The Optical Spectrum of 5145 Pholus. *Icarus* **99**, 238–240.

Birkett, C.M., S.F. Green, J.C. Zarkecki and K.S. Russell 1987. Infrared and Optical Observations of Low Activity Comets, P/Arend–Rigaux (1984k) and P/Neujmin 1 (1984c) *Mon. Not. R. astr. Soc.* **225**, 285–296.

Brown, W.R. and J.X. Luu 1997. CCD Photometry of the Centaur 1995GO. *Icarus* **126**, 218–224.

Buie, M.W. and S.J. Bus 1992. Physical Observations of (5145) Pholus. *Icarus* **100**, 288–294.

Campins, H., M.F. A'Hearn and L. McFadden 1987. The Bare Nucleus of Comet Neujmin 1. *Astrophys. J.* **316**, 847–857.

Campins H., C.M. Telesco, D.J. Osip, G.H. Rieke, M.J. Rieke and B. Schulz, 1994. The color temperature of (2060) Chiron — a warm and small nucleus. *Astron. J.* **108**, 2318–2322

Campins, H., D.J. Osip, G.H. Rieke and M.J. Rieke 1995. Estimates of the Radius and Albedo of Comet-Asteroid Transition Object 4015 Wilson-Harrington Based on Infrared Observations. *Planet. Space Sci.* **43**, 733–736.

Cruikshank, D., W.K. Hartmann and D.J. Tholen 1985. Color, Albedo and Nucleus Size of Halley's Comet. *Nature* **315**, 122–124.

Currie, 1992. Kappa-Kernal Application Package. Starlink User Note 95.8. Starlink project. CLRC/Rutherford Appleton Laboratory, Didcot, UK. http://star-www.rl.ac.uk.sun.html

Davies, J.K., M.V. Sykes and D.P. Cruikshank 1993a. Near Infrared Photometry and Spectroscopy of the Unusual Minor Planet 5145 Pholus (1992AD). *Icarus* **102**, 166–169.

Davies, J.K., J. Spencer, M.V. Sykes, D.J. Tholen and S.F. Green 1993b. *IAUC* 5698.

Davies, J.K., D.J. Tholen and D.R. Ballantyne 1996. Infrared Observations of Distant Asteroids. In *Completing the Inventory of the Solar System*, ASP Conference Proceedings (T.W. Rettig and J.M. Hahn, Eds.), **107**, pp. 97–105, ASP, San Francisco.

Davies, J.K., N. McBride and S.F. Green 1997. Optical and Infrared Photometry of Kuiper Belt Object 1993SC. *Icarus* **125**, 61-66.

Degewij, J., D. Cruikshank and W.K. Hartmann 1980. Near-infrared colorimetry of J7 Himalia and S9 Phoebe: a summary of 0.3 to 2.2 μm reflectances. *Icarus* **44**, 541–547.

Eaton, N. 1989. Photom-Aperture Photometry Routine. Starlink User Note 45.1. Starlink project. CLRC/Rutherford Appleton Laboratory,Didcot, UK. http://star-www.rl.ac.uk.sun.html

Fink, U., M. Hoffmann, W. Grundy, M. Hicks and W. Sears 1992. The Steep Red Spectrum of 1992AD: an Asteroid Covered with Organic Material? *Icarus* **97**, 145–149.

Hammergren, M. 1996. *IAUC* 6462.

Harris, A.W., J.W. Young, E. Bowell, L.J. Martin, R.L. Millis, M. Poutanen, F. Scaltriti, V. Zappala, H.J. Schober, H. Debehogne and K.W. Zeigler 1989. Photoelectric observations of asteroids 3, 24, 60, 261 and 863. *Icarus* **77**, 171–186.

Hartmann, W.K., D.P. Cruikshank and J. Degewij 1982. Remote Comets and Related Bodies: JHK Colorimetry and Surface Materials. *Icarus* **52**, 377–408.

Hartmann, W.K., D.J. Tholen, K.J. Meech and D.P. Cruikshank 1990. 2060 Chiron: Colorimetry and Cometary Behavior. *Icarus* **83**, 1–15.

Helin, E.F., S. Pravdo and K.J. Lawrence 1996. *MPEC* 1996-P03.

Jewitt, D. 1996. *IAUC* 6452.

Jewitt, D.C. and K.J. Meech 1988. The Optical Properties of Cometary Nuclei and a Preliminary Comparison With Asteroids. *Astrophys. J.* **328**, 974–986.

Keller H.U., W. Curdt, J.-R. Kramm and N. Thomas, 1994. In *Images of the Nucleus of Comet Halley* (R. Reinhard, N. Longdon and B. Battrick B., Eds.), ESA SP-1127.

Landolt, A.U. 1992. UBVRI photometric standard stars in the magnitude range 11.5<V<16.0 around the celestial equator. *Astron. J.* **104**, 340–371.

Lasker, B.M., C.R. Sturch, C. Lopez, A.D. Mallama, S.F. McLaughlin, J.L. Russel, W.Z. Wisniewski, B.A. Gillespie, H. Jenker, E.D. Siciliano, D. Kenny, J.H. Baumert, A.M. Goldberg, G.W. Henry, E. Kemper and M.J. Siegel 1988. The Guide Star Photometric Catalog. I. *Astrophys. J. Suppl.* **68**, 1–90.

Lebofsky, L.A., D.J. Tholen, G.H. Rieke and M.J. Lebofsky 1984. 2060 Chiron:Visual and Thermal Infrared Observations. *Icarus* **60**, 532–537.

Luu J.X. 1993. Spectral Diversity Among the Nuclei of Comets *Icarus* **104**, 138–148.

Luu J.X. 1994. The Kuiper Belt. In *Asteroids Comets Meteors 1993*, (A. Milani, M. Di Martino and A. Cellino, Eds.), Kluwer, pp. 31–44.

Luu, J., D. Jewitt and E. Cloutis 1994. Near Infrared Spectroscopy of Primitive Solar System Objects. *Icarus* **109**, 133–144.

Meech, K.J., Knopp, G.P. and Farnham, T.L., 1995, The split nucleus of comet Wilson (C/1986P1=1887VII), *Icarus*, **116**, 46–76.

Millis, R.L., M.F. A'Hearn and H. Campins 1988. An investigation of the Nucleus and Coma of Comet P/Arend-Rigaux. *Astrophys. J.* **324**, 1194–1209.

Mottola, S. and U. Carsenty, 1996. *IAUC* 6472.

Mueller, B.E.A., D.J. Tholen, W.K. Hartmann and D. Cruikshank, 1992. Extraordinary colors of asteroidal object (5145 Pholus) 1992AD. *Icarus* **97**, 150–154.

Rabinowitz, D.L. 1996. *IAUC* 6466.

Romaniskin, W., S.C. Tegler, J. Levine and N. Butler, 1997. BVR photometry of Centaur objects 1995GO, 1993HA$_2$ and 5145 Pholus. *Astron. J.* **113**, 1893–1898.

Thomas N. and H.U. Keller 1989. The Colour of Comet P/Halley's Nucleus and Dust. *Astron. & Astrophys.* **213**, 487–494.

Tokunaga A.T. and M.S. Hanner 1985. Does Comet P/Arend–Rigaux have a large, dark nucleus? *Astrophys. J.* **296**, L13–16.

Weintraub, D.A., S.C. Tegler, W. Romanishin 1997. Visible and near Infrared Photometry of the Centaur Objects 1995GO and 5145 Pholus. *Icarus* in Press

Williams, G. 1996. *IAUC* 6452.

Williams, I.P., M. Cartwright and A. Fitzsimmons 1996. *IAUC* 6469.

TABLE I

1996PW Observations

UT Date	r AU	Δ AU	$\alpha°$	Telescope	Observer	Note
1996 Aug 23	2.540	1.532	2.3	UKIRT	JKD	K spectrum
1996 Sep 04	2.551	1.565	6.1	UKIRT	SKL (UKIRTSERV)	JHK photometry
1996 Sep 07	2.555	1.580	7.2	Bochum	SM, UC	R lightcurve
1996 Sep 08	2.557	1.585	7.6	Bochum	SM, UC	R lightcurve, V photometry
1996 Sep 09	2.558	1.591	8.0	Bochum	SM, UC	R lightcurve
1996 Sep 10	2.560	1.597	8.4	Bochum	SM, UC	R lightcurve, V photometry
1996 Sep 10	2.560	1.597	8.4	UKIRT	TGH	JHK photometry
1996 Sep 12	2.563	1.610	9.1	UKIRT	LM	K photometry
1996 Sep 29	2.595	1.755	14.7	UKIRT	JKD	K spectrum
1996 Oct 11	2.626	1.892	17.5	INT	JKD, NM, KAH	VRI photometry
1996 Oct 12	2.629	1.905	17.7	INT	JKD, NM, KAH	VRI photometry
1996 Oct 13	2.631	1.918	17.9	INT	JKD, NM, KAH	VRI photometry
1996 Oct 23	2.662	2.052	19.4	UKIRT	TK, (UKIRTSERV)	JHK photometry
1996 Oct 29	2.682	2.138	20.0	UKIRT	JKD, DB	JHK photometry
1996 Oct 30	2.685	2.153	20.1	UKIRT	JKD, DB	JHK photometry

Note. The aspect data given for each date is for 00^{h} UT. The JHK photometry on 1996 Oct 29 and 30 were calibrated on the 31st.

TABLE II

Lightcurve data from ESO/Bochum

MJD	Relative R	V(1,α = 7.6°)	MJD	Relative R	V(1,α = 7.6°)
50332.98450	−5.640	14.635	Cont...		
50333.02972	−5.623	14.651	50335.05559	−5.404	14.809
50333.05646	−5.679	14.594	50335.07984	−5.473	14.739
50333.08109	−5.691	14.582	50335.10366	−5.477	14.735
50333.10674	−5.747	14.525	50335.12693	−5.491	14.720
50333.13301	−5.711	14.561	50335.15478	−5.556	14.655
50333.15558	−5.744	14.527	50335.17642	−5.617	14.594
50333.17696	−5.748	14.523	50335.20172	−5.610	14.600
50333.19945	−5.740	14.530	50335.22652	−5.626	14.584
50333.22373	−5.737	14.533	50335.25046	−5.634	14.575
50333.24692	−5.745	14.524	50335.27799	−5.645	14.563
50333.26945	−5.721	14.548	50335.29993	−5.688	14.520
50333.29298	−5.664	14.604	50335.31784	−5.671	14.537
50333.31533	−5.653	14.615	50335.33473	−5.697	14.510
50333.33277	−5.623	14.645	50335.98173	−5.562	14.633
50333.97527	−5.702	14.532	50336.00901	−5.587	14.607
50333.99098	−5.702	14.532	50336.02580	−5.585	14.609
50334.01906	−5.680	14.554	50336.04187	−5.625	14.569
50334.04418	−5.664	14.569	50336.06658	−5.643	14.550
50334.06798	−5.646	14.587	50336.09125	−5.652	14.541
50334.09191	−5.584	14.648	50336.10948	−5.671	14.521
50334.11873	−5.516	14.716	50336.12816	−5.662	14.530
50334.15486	V=17.809±0.03	14.769	50336.14916	−5.645	14.546
50334.17935	−5.379	14.851	50336.16829	V=17.644±0.03	14.545
50334.20204	−5.377	14.853	50336.18664	−5.674	14.517
50334.22553	−5.341	14.888	50336.20507	−5.645	14.545
50334.25250	−5.332	14.897	50336.22142	−5.626	14.564
50334.27435	−5.377	14.851	50336.24402	−5.628	14.562
50334.29769	−5.407	14.821	50336.26115	−5.569	14.620
50334.32138	−5.380	14.848	50336.27314	−5.560	14.629
50334.99198	−5.277	14.937	50336.29048	−5.517	14.672
50335.02676	−5.402	14.811	50336.30927	−5.547	14.641

Note. The MJD dates are mid-frame light-time corrected times. All frames had exposures of 100 s. Typical errors for all final magnitudes are ± 0.03. The relative R data shown here has then been phase-corrected assuming G=0.05 (see text) to a phase of 7.6° (as at 50334.0 MJD), reduced to $r = \Delta = 1$ AU and calibrated to the V frames to produce the final V($1,\alpha = 7.6°$) magnitudes. The two calibrated V frames are indicated.

TABLE III

Mass production rates for 1996PW determined from image profile fitting

Pixel Distance	$r_\circ$ (m)	$\dot{M}$(star 1) (g s^{-1})	$\dot{M}$(star 2) (g s^{-1})	$\dot{M}$(star 3) (g s^{-1})	$\dot{M}$(star 4) (g s^{-1})
3.5	2.9×10^6	58±7	10±8	−4±8	−31±8
4.5	3.7×10^6	61±7	28±8	31±8	18±8
5.5	4.5×10^6	28±7	8±8	23±8	9±8
6.5	5.3×10^6	12±9	4±10	7±10	0±10
7.5	6.2×10^6	31±9	26±10	30±10	23±10
8.5	7.0×10^6	20±10	0±11	21±11	15±11
9.5	7.8×10^6	12±11	−3±12	10±12	−7±12
10.5	8.6×10^6	27±11	13±13	19±13	13±13
11.5	9.5×10^6	27±13	12±15	22±15	24±15
12.5	1.0×10^7	24±13	7±14	25±14	13±14
13.5	1.1×10^7	21±13	−4±15	28±15	29±15
14.5	1.2×10^7	14±14	6±16	17±16	8±16
Mean:		28	9	19	10

Note. The errors qutoed for the $\dot{M}$ values are determined from the combined photon statistical errors for the 1996PW and test star profiles.

TABLE IV

Optical Photometry from the INT

MJD	Filter	Exp (s)	Mag	Mag(1,$\alpha = 17.9°$)
50367.93750	R	60	17.992±0.04	14.490
50367.94141	I	60	17.479±0.06	13.983
50367.94141	V	60	18.602±0.05	15.100
50367.96094	R	60	18.054±0.04	14.551
50367.97266	V	240	18.625±0.04	15.121
50367.97656	I	240	17.720±0.05	14.222
50367.98047	R	180	18.115±0.03	14.611
50368.91797	R	300	18.538±0.03	15.024
50368.92578	V	300	19.080±0.04	15.566
50368.92969	I	300	18.081±0.06	14.567
50368.96094	I	300	18.057±0.05	14.543
50368.96875	R	300	18.426±0.03	14.912
50368.97266	V	300	19.021±0.03	15.507
50368.97656	I	300	17.893±0.05	14.379
50368.98438	V	500	18.982±0.03	15.468
50368.99219	R	500	18.432±0.03	14.923
50369.00000	R	500	18.357±0.03	14.842
50369.87109	V	500	18.780±0.03	15.255
50369.87891	R	500	18.146±0.03	14.621
50369.88672	I	500	17.788±0.05	14.258
50369.93359	R	500	18.141±0.03	14.615
50369.94141	V	500	18.659±0.03	15.133
50369.94922	I	400	17.557±0.05	14.027
50369.95313	I	300	17.485±0.05	13.954

Note. The MJD dates are mid-frame light-time corrected times. The magnitudes shown here have then been phase-corrected assuming G=0.05 (see text) to a phase of 17.9° (as at 50369.0 MJD) and reduced to $r = \Delta = 1$ AU to produce the final Mag(1,$\alpha = 17.9°$) magnitudes.

TABLE V

Infrared photometry from UKIRT

UT Date	Filter	IR mag.	Lightcurve phase	V(1,α)	V used	V$-$(IR mag)
Sep 04.30766	J	15.62$\pm$0.01	0.79075	14.558	17.492	1.87$\pm$0.04
Sep 04.31553	H	15.27$\pm$0.01	0.79608	14.568	17.502	2.23$\pm$0.04
Sep 04.33455	K	15.23$\pm$0.02	0.80896	14.594	17.528	2.30$\pm$0.05
Sep 10.48791	J	16.25$\pm$0.01	0.97601	14.920	18.029	1.78$\pm$0.04
Sep 10.49059	H	15.85$\pm$0.02	0.97783	14.918	18.027	2.18$\pm$0.05
Sep 10.50552	K	15.84$\pm$0.02	0.98794	14.888	17.997	2.16$\pm$0.05
Sep 12.40793	K	15.36$\pm$0.02	0.27625	14.538	17.701	2.34$\pm$0.05
Oct 23.32685	J	17.49$\pm$0.03	0.98652	15.45	19.198	1.71$\pm$0.05
Oct 23.33518	H	16.94$\pm$0.04	0.99216	15.44	19.189	2.25$\pm$0.06
Oct 23.34360	K	16.62$\pm$0.07	0.99786	15.42	19.169	2.55$\pm$0.08
Oct 29.18143	J	17.58$\pm$0.03	0.95124	15.532	19.406	1.83$\pm$0.05
Oct 29.19131	J	17.66$\pm$0.03	0.95793	15.528	19.402	1.74$\pm$0.05
Oct 29.20042	H	17.31$\pm$0.08	0.96409	15.52	19.394	2.08$\pm$0.09
Oct 29.21181	K	17.03$\pm$0.14	0.97181	15.50	19.374	2.34$\pm$0.14
Oct 29.22070	J	17.59$\pm$0.03	0.97783	15.49	19.364	1.77$\pm$0.05
Oct 29.27226	J	17.42$\pm$0.03	0.01274	15.372	19.247	1.83$\pm$0.05
Oct 29.27966	H	17.03$\pm$0.08	0.01775	15.36	19.235	2.21$\pm$0.09
Oct 29.28728	K	17.01$\pm$0.14	0.02291	15.348	19.223	2.21$\pm$0.14
Oct 29.29481	J	17.42$\pm$0.03	0.02802	15.29	19.165	1.75$\pm$0.05
Oct 30.18495	K	16.74$\pm$0.07	0.63082	15.20	19.094	2.35$\pm$0.08
Oct 30.19776	H	16.88$\pm$0.03	0.63949	15.188	19.083	2.20$\pm$0.05
Oct 30.20707	J	17.21$\pm$0.02	0.64580	15.18	19.075	1.87$\pm$0.05
Oct 30.21561	H	16.91$\pm$0.03	0.65158	15.17	19.065	2.16$\pm$0.05
Oct 30.22404	J	17.23$\pm$0.02	0.65729	15.16	19.055	1.83$\pm$0.05

Note. The UT dates are mid-frame light-time corrected times. Exposure times were 9 minutes for each observation except for September 10 which were 4 minutes. To obtain a V$-$IR color, a V is derived from the lightcurve shown in Fig. 1b at the appropriate lightcurve phase, and converted to the correct r, Δ and α of the IR observation. For the September observations, the actual lightcurve is used (Fig. 1a); for the October observations, the V fit (Fig. 1b); this is to minimise the error in the correction for phase angle. When correcting for phase angle, G=0.05 is used (see text).

TABLE VI

Optical–Infrared Colors of Solar System Objects

Object	Group	B−V	V−R	V−I	V−J	V−H	V−K	Albedo
1993SC	KBO		0.54±0.14[a]	0.97±0.14[a]	2.08±0.15[a]			
95P/Chiron	CEN	0.70±0.02[b]	0.38±0.03[c1]	0.72±0.03[c1]	1.11±0.04[c2]	1.42±0.04[c2]	1.45±0.04[c2]	∼0.13[d]
			0.39±0.03[c2]	0.71±0.04[c2]	1.18±0.04[c3]	1.43±0.04[c3]	1.48±0.04[c3]	$0.14^{+0.06}_{-0.03}$[e]
			0.34±0.03[c3]	0.62±0.03[c3]	0.89±0.15[f]	1.34±0.2[f]	1.36±0.2[f]	
			0.34±0.03[c4]					
5145 Pholus	CEN	1.35[g2]	0.75[g1]	1.51[g1]	2.46±0.2[h]	2.91±0.2[h]	2.87±0.2[h]	<0.044±0.013[i]
			0.66[g2]	1.34[g2]	2.67±0.2[o]	2.97±0.2[o]	3.01±0.2[o]	
			0.810±0.006[j]					
			0.81±0.02[k]	1.68±0.05[k]				
			0.78±0.02[l]	1.62±0.03[l]				
7066 Nessus	CEN		0.77±0.05[m]		2.07±0.09[n]		2.28±0.07[n]	
1995GO	CEN	0.75±0.04[m]	0.47±0.04[m]		1.72±0.30[o]	2.15±0.30[o]	2.39±0.31[o]	
		0.73±0.04[p]	0.78±0.05[p]					
1P/Halley	COM	0.73±0.03[q]	0.44±0.03[q]	0.92±0.07[q]	1.66±0.19[r]		2.31±0.19[r]	∼0.04[s]
28P/Neujmin 1	COM	0.86±0.04[t]	0.41±0.03[t]	0.99±0.04[t]	1.66±0.06[t]	2.06±0.06[t]	2.15±0.05[t]	0.02–0.03[t]
			0.50±0.04[u]					
49P/Arend-Rigaux	COM		0.47±0.01[v]	0.98±0.02[v]	1.63[w]	1.99[w]	2.13[w]	0.054±0.01[x]
								0.06±0.03[y]
29P/Schwassmann Wachmann 1	COM				1.73±0.13[f]	2.23±0.20[f]	2.07±0.21[f]	
4015 Wilson-Harrington	COM/AST				1.06[f]	1.34[f]	1.61[f]	0.05±0.01[z]
1996PW	—		0.56±0.04	1.03±0.06	1.80±0.05	2.19±0.05	2.32±0.05	

TABLE VI (continued)

Note. Refs: [a]Davies *et al.* (1997); [b]Lebofsky *et al.* (1984); [c]Hartmann *et al.* (1990), (1) 1988 Feb 20, (2) 1988 Feb 21, (3) 1988 Feb 22, (4) 1988 Sep 9. [d] Altenhoff & Stumpff (1995); [e]Campins *et al.* (1994); [f]Hartmann *et al.* (1982); [g]Mueller *et al.* (1992), (1) 1992 Jan 9, (2) 1993 Jan 23; [h]Davies *et al.* (1993a); [i]Davies *et al.* (1993b); [j]Buie & Bus (1992); [k]Fink *et al.* (1992) deduced here from their reflectance spectrum; [l]Binzel *et al.* (1992) deduced here from their reflectance spectrum; [m]Romaniskin *et al.* (1997) [n]Davies *et al.* (1996); [o]Weintraub *et al.* (1997); [p]Brown & Luu (1997); [q]Thomas & Keller (1989) deduced here from their reflectivity gradients; [r]Cruikshank *et al.* (1985); [s]Keller *et al.* (1994); [t]Campins *et al.* (1987) deduced here from their reflectance spectrum; [u]Jewitt & Meech (1988); [v]Luu (1993) deduced here from their reflectivity gradients; [w]Millis *et al.* (1988) no error quoted; [x]Tokunaga & Hanner (1985) albedo at 1.25 μm; [y]Birkett *et al.* (1987) albedo at 1.25 μm; [z]Campins *et al.* (1995)